Ceramics International 43 (2017) 16416–16423

Contents lists available at ScienceDirect

Ceramics International

journal homepage: www.elsevier.com/locate/ceramint

Deposition of graded SiO_2/SiC coatings using high-velocity solution plasma spray

F.S. Miranda[a,*], F.R. Caliari[a], T.M. Campos[a], A.M. Essiptchouk[b], G.P. Filho[a]

[a] Centro de Ciência e Tecnologia de Plasmas e Materiais – PlasMat, Instituto Tecnológico de Aeronáutica – ITA, São José dos Campos 12228-900, SP, Brazil
[b] São Paulo State University – Unesp, Instituto de Ciência e Tecnologia, São José dos Campos 12247-004, SP, Brazil

ARTICLE INFO

Keywords:
Solution plasma spray
Supersonic plasma torch
Ceramic coatings
Graded coatings

ABSTRACT

Carbon/carbon (C/C) composites are widely used in structural components, particularly in the aerospace and aeronautics sectors. However, the application of C/C composites is limited by low oxidation resistance at high temperatures. In order to overcome this problem, graded SiO_2/SiC coatings were deposited on C/C composites by a high-velocity solution plasma spray (HVSPS) process. Graded coatings were formed by reactions between the $Si(OH)_4$ sprayed liquid precursor and the C/C substrate; these reactions were promoted by the high temperature of the plasma torch. The morphologies, microstructures, and chemical compositions of the coatings were investigated by X-ray diffraction, Raman spectroscopy, Fourier-transform infrared spectroscopy, and scanning electron microscopy/energy-dispersive X-ray spectroscopy. By altering the deposition time, the coating thickness was controlled, therefore demonstrating SiC formation and realizing graded SiO_2/SiC coatings.

1. Introduction

Carbon fiber-reinforced carbon (C/C) composites are suitable for use in structural components, especially those exposed to intense aerothermal loads, because they exhibit high strength, toughness, and thermal conductivity at high temperatures [1]. The high strength and exceptional fracture toughness of C/C composites, combined with their refractory properties and their resistance to erosion, corrosion, and wear, make these materials ideal for high-temperature structural components in advanced gas-turbine engines and reentry vehicles. When utilized in inert atmospheres or under vacuum, C/C composites maintain their mechanical properties at temperatures exceeding 2000 °C [2]. However, carbon has low oxidation resistance because it is highly reactive with oxygen and dissociated hydrogen, significantly hindering use in aerospace vehicles [3]. This problem can be overcome by the deposition of a coating that protects the C/C composite from oxidation and loss of mass, and thereby preserving the mechanical properties of the composite [4]. Lee [5] describes the basic principles for selecting the coating material: it must withstand reactive environments, possess low oxygen permeability and thus inhibit oxygen transport to the substrate, and be chemically compatible with the substrate. According to Webster et al. [2], oxide formation minimizes carbon diffusion outward from the substrate and prevents oxygen entry into the substrate. Materials with self-healing abilities could effectively protect the substrate; in this sense, glass or glass-forming material layers and coatings are extremely important in sealing cracks. Coatings with these characteristics can be classified as environmental barrier coatings (EBC) [6–8]. Silica (SiO_2) fulfills these requirements as an oxide with self-healing characteristics and low oxygen permeability that could prevent the external diffusion of carbon. Generally, C/C composites are coated with ceramics with variable thermal conductivities; materials with low thermal conductivity are used in aerospace applications to absorb part of the thermal energy encountered in use. This energy is utilized during oxidation reactions occurring upon atmospheric re-entry; for this reason, silicon-containing coatings are widely used [9]. The oxidation of silicon-based ceramics generates uniform, dense, low-oxygen-permeability SiO_2 glass films at high temperatures, providing good oxidation protection for C/C composites [10]. Therefore, several works have reported on the addition of SiO_2 to ceramic coatings. Yao et al. [11] deposited coatings of SiC–Si–ZrB_2 on C/C composites and performed oxidation tests. They observed glassy SiO_2 formation, which aided in filling cracks and directly prevented the oxidation of the substrate. Other studies also reported the formation of ZrO_2 formed by the oxidation of ZrB_2, which reacts with SiO_2 to form $ZrSiO_4$. The high thermal stability of $ZrSiO_4$ reduces SiO_2 consumption, which improves the oxidation resistance [12]. Oxidation resistance can be increased by dispersing SiC in ZrB_2 coatings, thereby increasing the interfacial area between materials. The addition of SiC promotes the formation of SiO_2 glass in the coating, which decreases the permeability of oxygen to the substrate and ensures protection against oxidation [13]. For coating C/

* Corresponding author.
E-mail address: mirannda.fs@gmail.com (F.S. Miranda).

http://dx.doi.org/10.1016/j.ceramint.2017.09.018
Received 15 June 2017; Received in revised form 17 August 2017; Accepted 2 September 2017
Available online 06 September 2017

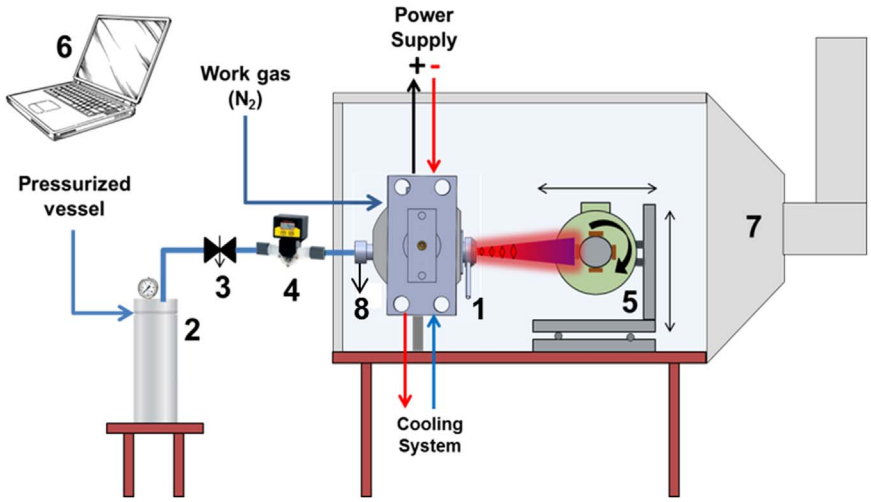

Fig. 1. Schematic of HVSPS system: (1) Tandem-type plasma torch, (2) pressurized vessel, (3) needle valve, (4) solution flowmeter, (5) dynamic sample holder, (6) control and data acquisition system, (7) exhaust system, and (8) atomizer nozzle.

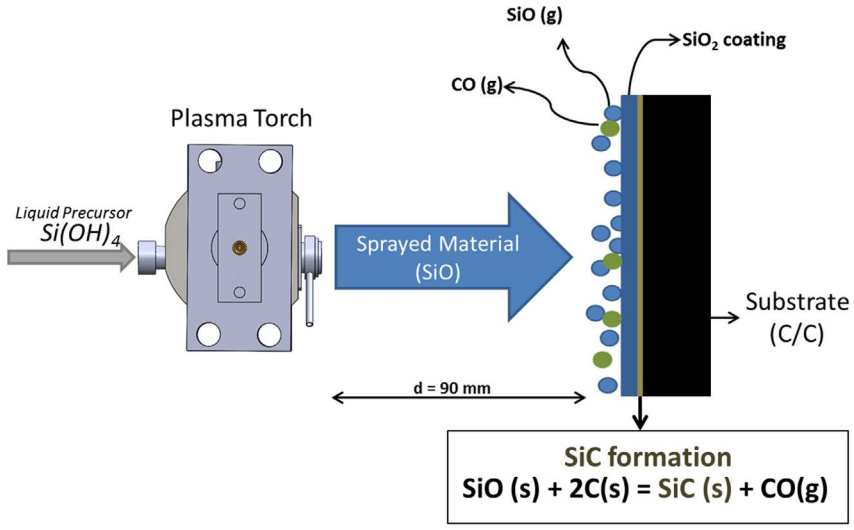

Fig. 2. SiC formation during HVSPS process.

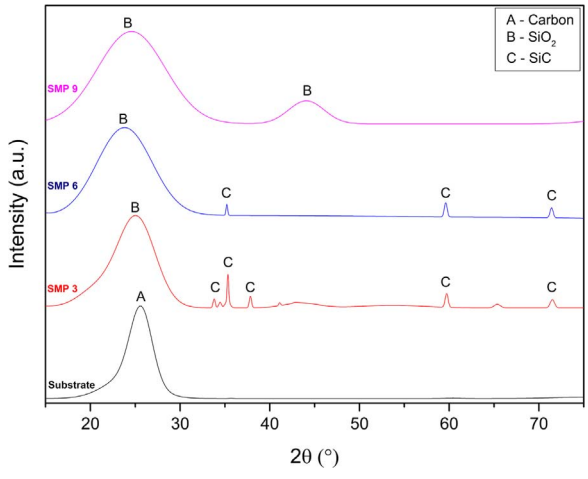

Fig. 3. XRD patterns of substrate and coatings obtained via HVSPS process.

C composites, bond coating is necessary; SiC is the most widely used material for bond coatings because it is highly physically and chemically compatible with C/C composites. The bond-coating procedure is performed to reduce the appearance of cracks in the coating. However, during layer deposition, voids can form between the bond coat and the top coat, reducing the stability and substrate protection of the coating [14]. Several techniques are used to deposit coatings, including chemical vapor deposition, pack cementation, hydrothermal electrophoretic deposition, slurry methods, and plasma spraying [15]. Among these, the plasma spraying technique has high application potential because it offers flexibility in processing many material types, few geometric restrictions on the substrate shape, and high deposition rates [16]. Solution plasma spraying (SPS) uses liquid precursors containing either the final coating composition or main elements thereof that react with the substrate, the plasma gas, or the surrounding atmosphere. SPS allows creates materials with nanoscale grain sizes, correlating to lower defect indices, higher strain tolerances, and better porosity distributions, which reduce the thermal conductivity and elasticity modulus, particularly in ceramic materials [17–19]. In addition, the reactivity of the plasma can be exploited by combining the plasma spraying process with one-step materials synthesis, thereby creating coatings with chemical graduation [20–22]. Reactive plasma spraying can produce in-situ composite coatings through reactions among two or more materials [23]. This work describes the experimental results obtained in the deposition of SiO_2/SiC graded coatings formed from reactions between sprayed SiO and the C/C composite substrate. SiC formation at atmospheric pressure has not yet been reported; it occurred in this study because of the characteristic of the high-velocity SPS (HVSPS) process. This process enabled the deposition of an efficient SiO_2/SiC graded EBC without requiring a SiC bond coat and thereby preventing void

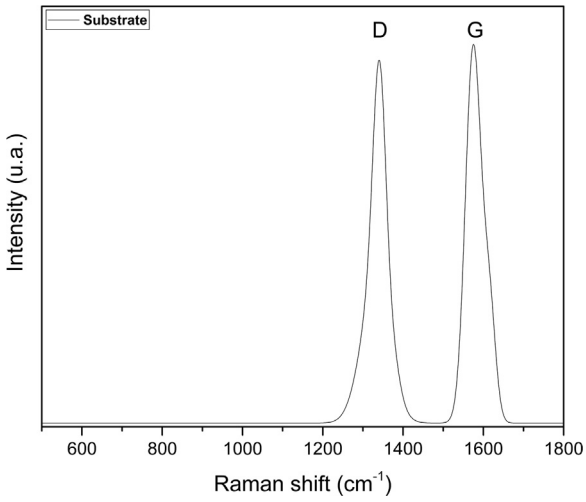

Fig. 4. Raman spectrum of C/C substrate.

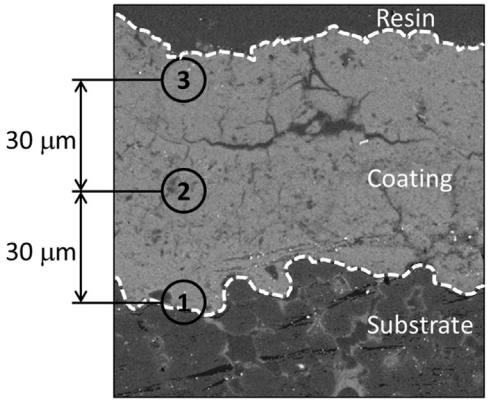

Fig. 5. Locations for coating composition gradient analysis: (1) Substrate/coating interface, (2) intermediate region of coating, and (3) top of coating.

formation between the interlayer and coating, because the deposition process occurred in a single step. The obtained microstructures, chemically graded compositions, and properties of the coatings, such as self-healing characteristics, were investigated and the results discussed.

2. Materials and methods

2.1. Liquid precursor of silica

Silicic acid ($Si(OH)_4$) was obtained by passing 10 wt% aqueous sodium metasilicate ($Na_2SiO_3{\cdot}5H_2O$) through an ion-exchange resin (IR-120; Rohm and Haas).

2.2. Preparation of SiO_2 coatings on C/C composites

Depositions were performed by HVSPS on a C/C composite substrate developed by the materials group of the Institute of Aeronautics and Space (IAE/DCTA). The C/C composites were obtained from prepregs of carbon fiber and phenolic resins with a density of approximately 1.78 g/cm^3, cut into 20 × 15 × 4 mm blocks, sanded at the edges to remove irregularities, and cleaned. The experimental system, described in detail by Caliari et al. [24], originally comprised a supersonic plasma torch with axial injection, powder injection system, cooling subsystems, electric power source, and gas supply. However, for processing the liquid precursor, certain adaptations were made to the transportation line; a pressurized vessel of 0.001 m^3 in capacity was added, as were a needle valve and flow meter connected to an atomizer nozzle coupled directly with the plasma torch. In order to distinguish the two systems, the former is referred to as HVSPS. A dynamic sample holder with three-dimensional (3D) position and rotation control with the capacity to process eight samples simultaneously was used. Fig. 1 shows a schematic of the experimental system.

Experiments were performed with the N_2 working gas flow rate of 270 L/min, while the liquid precursor flow rate was 80 mL/min. The depositions were performed at the stand-off distance of 90 mm from the plasma torch nozzle; the samples were rotated at 80 rpm. The operating parameters of the plasma torch were fixed at the current and voltage of 100 A and 340 V, respectively. All samples were preheated to 200 °C before starting the deposition process. Three experiments with eight samples treated simultaneously were performed with constant distance and varied deposition times of 3, 6, and 9 min. The deposition time directly affected the coating thickness. The samples were identified according to the exposure times, i.e., SMP3, SMP6, and SMP9.

The crystalline structures of the substrates and obtained coatings were investigated by X-ray diffraction (XRD) using an X'Pert Powder diffractometer (Panalytical), with a step size of 0.02°, 2θ range of 15–100°, and step time of 10 s. Raman scattering spectroscopic analysis was employed to determine the chemical compositions of the substrate and coatings using a Renishaw 2000 spectrometer (Renishaw), with excitation wavelengths in the visible spectrum (532 nm) and two accumulations. In addition, Fourier-transform infrared (FTIR) spectroscopy by a Perkin Elmer Frontier apparatus using universal attenuated total reflectance (UATR) was performed with 16 accumulations. The coating microstructures were observed by a Vega 3 XMU (Tescan) scanning electron microscope (SEM). Cross-sections of the samples were prepared following conventional metallographic procedures.

3. Results and discussions

3.1. Reactions between sprayed material and substrate

SiO_2 coatings were deposited on the C/C composite substrates without using bond coatings. The deposition of the bond coating could reduce substrate–coating incompatibility and thereby prevent detachment, as reported by Yang et al. [25]. This procedure was unnecessary with HVSPS, because the process promoted SiC formation through reactions between the sprayed material and substrate at atmospheric pressure with a substrate temperature of ~ 350 °C. Qi et al. [26] presented a similar SiC formation reaction, but obtained SiC by a carbothermal chemical vapor deposition method to cover carbon nanotubes with SiC layers. Gundiah et al. [27] described a SiC formation reaction using a controlled atmosphere of NH_3 or H_2 in which silica gel was mixed with activated carbon; the reactions occurred at 1360 °C in a period of 4–7 h. Allaire et al. [28] described an experimental procedure for SiC powder production using a radially injected DC plasma torch that initiated the reaction between gaseous silicon tetrachloride and methane. Fig. 2 shows schematically the SiC formation reaction in this experiment, which occurs by SiO diffusion on the C/C substrate during the HVSPS deposition process.

3.2. Substrate and coatings characterizations

Fig. 3 shows the XRD patterns of the substrate and coatings obtained by the HVSPS process. In comparing the patterns, that from the substrate contains only a peak at the carbon-related diffraction angle (25°), while those from the coated samples show peaks of SiO_2 (22°) and SiC (35°) [29,30]. The formation of the SiC is evident from the pattern of sample SMP3. The prevalence of the SiC coating is inversely related to the coating thickness; with a thinner coating, the formed SiC becomes more visible in XRD analysis. The pattern of the sample receiving 6 min of deposition (SMP6) lacks some SiC peaks because of the increased coating thickness. In the sample processed for 9 min (SMP9) all SiC-related peaks are gone from the diffraction pattern, leaving only the

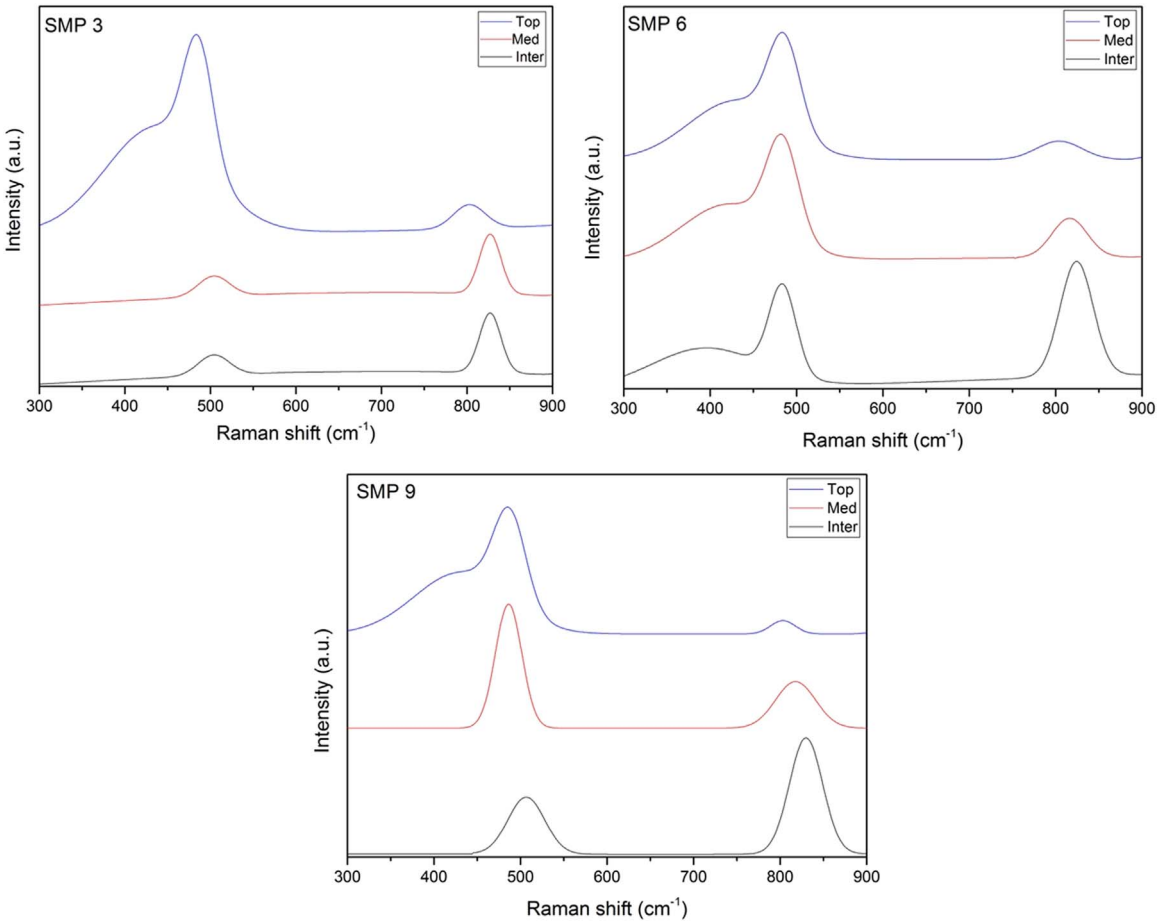

Fig. 6. Raman spectra of the coated samples obtained from (1) substrate/coating interface, (2) intermediate region of coating, and (3) top of coating. (For interpretation of the references to color in this figure legend, the reader is referred to the web version of this article.)

SiO_2-related peak, which is present in the patterns of all the samples that received deposition. The obtained SiO_2 coating is amorphous in structure, as observed by the halo located at approximately 22°, from the transformation and organization characteristics of silica, which are highly affected by the heating and cooling rates. Rapid cooling of ceramics, such as SiO_2, is often used to obtain non-crystalline materials; the rapid heating promotes incomplete reactions, causing the nucleation of amorphous glass [31,32]. Furthermore, nanoscale particle formation, characteristic of the SPS technique, during precursor processing also affects the non-crystallization of silica; [18,33,34]. Finally, the supersonic plasma jet regime promotes a small residence time for the material during processing; the heating and cooling by the jet is fast enough to inhibit crystallization [35,36].

3.2.1. Graded composition

Fig. 4 shows the Raman spectrum of the C/C substrate. Two peaks are located at 1340 cm^{-1} and 1590 cm^{-1}, corresponding to the D and G bands respectively, characteristic of carbon-based materials [37].

In order to identify the compositional gradient of the coating, Raman analyses were made at three points over the cross-section. Points 1, 2, and 3 were located at the substrate/coating interface, an intermediate region of the coating, and the top of the coating, respectively, as shown in Fig. 5.

Fig. 6 shows the Raman spectra obtained from the coated samples. In all samples, regardless of deposition time, the spectra obtained from point 1 (black line) show lower intensity of the Si–O–Si bond peak at approximately 500 cm^{-1} than those at points 2 (red line) and 3 (blue line). The opposite trend occurs for the Si–C bond peak located at approximately 820 cm^{-1}; it decreases in intensity from points 1–3. These results demonstrate that the reaction between the sprayed material and the C/C substrate causes a coating gradient of Si–O and Si–C. The substrate/coating interface has a higher concentration of Si–C; along the coating cross-section, the Si–C concentration decreases while the Si–O concentration increases, as the predominant material of the coating. The formation of SiC occurs by reactions between the substrate and coating precursor, contributing to the increased chemical compatibility between the substrate and coating [38].

Fig. 7 shows the FTIR spectra of SMP3, SMP6, and SMP9 obtained in absorbance mode. In all spectra, four vibration modes are apparent. The principal band located at ~ 1050 cm^{-1} relates to Si–O stretching (c), that at ~ 950 cm^{-1} to Si–O binding (b), and that at 1200 cm^{-1} to Si–O defects (d). These defects are formed mainly by the presence of oxygen at the SiO_2/SiC interface [39,40]. The band located at ~ 800 cm^{-1} relates to the Si–C bond [41]; the presence of the band confirms the formation of SiC during deposition. SiC formation is associated with the partial reduction of silica; as the area of the main peak of SiO (c) decreases, that of SiC (a) increases. Because the relative intensities or relative integrated areas of the absorbance peaks in curve-fitted FTIR spectra are proportional to the concentrations of given materials [42], the increase in SiC formation can be determined by the proportion of the areas of the main absorption peaks of SiO (c) and SiC (a) using Eq. (1):

$$\frac{A_{SiC}}{A_{SiC} + A_{SiO}} \quad (1)$$

where A_{SiC} is the total area of the SiC absorption band and A_{SiO} is that of SiO.

From this equation, the proportions of the areas of each deposited

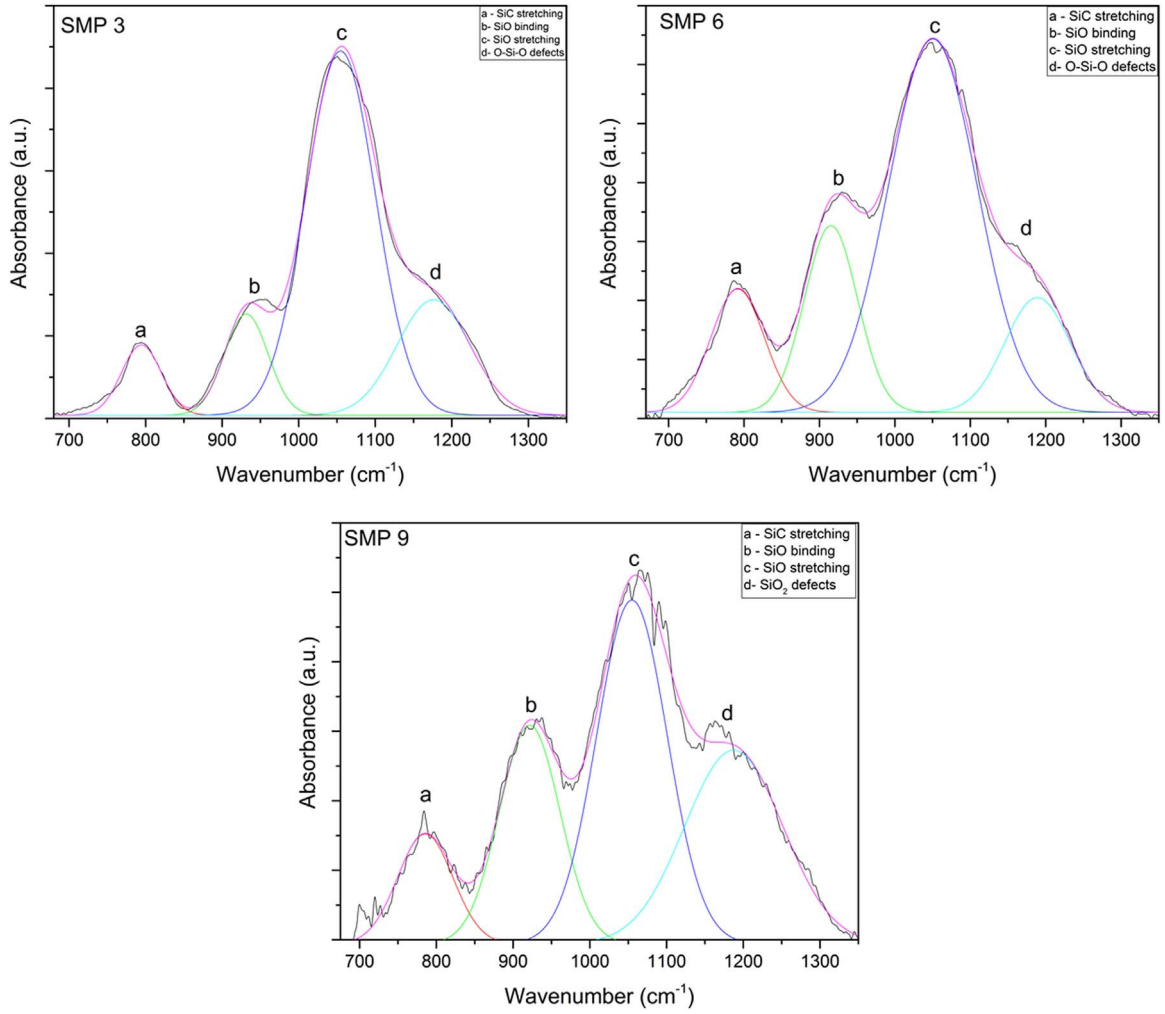

Fig. 7. FTIR absorbance spectra of SMP3, SMP6, and SMP9.

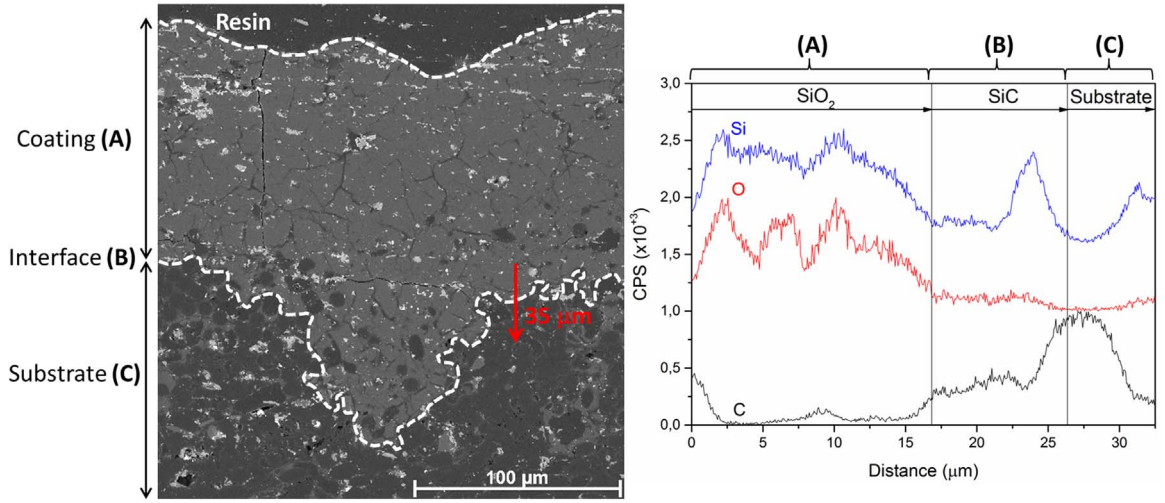

Fig. 8. SEM image of cross-section of SMP9 and EDS results showing the composition of coating (A), interface (B), and substrate (C).

sample were calculated. For SMP3, SMP6, and SMP9, the ratios between the areas were 0.1, 0.16, and 0.2, respectively. This indicates that, with increased deposition time and consequently plasma jet exposure, the reactions forming Si–C bonds are enhanced, confirming the results obtained by Raman and XRD analysis showing the gradient coatings. Similarly, the area of the SiO_2/SiC interfacial defect band (d) increases. This demonstrates that, with increased coating thickness, the oxygen concentration increases, directly causing the increase in the defect band (d) from the greater number of Si–O bonds.

Table 1
Coatings thickness.

Sample	Coating thickness [μm]
SMP 3	40
SMP 6	80
SMP 9	120

3.3. Microstructure of SiO_2 coatings

Fig. 8 presents SEM images from the cross-section of SMP9 and the energy-dispersive X-ray spectroscopy (EDS) results obtained from line-scanning mode to verify the chemical composition of the coatings and interface. The coatings contain Si and O, as shown in region A. The substrate/coating interface shows Si and C; these results are expected because of the gradient nature of the coatings. The deposited material is observed to penetrate the interior of the substrate, potentially providing protection against oxidation by filling voids between the fibers of the composite.

In analyzing the coating microstructure (Fig. 8), defects are observed such as vertical cracks. These may not deteriorate the coating performance because silica is self-healing, able to fill such cracks upon high-temperature exposure [43]. This ensures that, under high-temperature and oxidative environments, vertical cracks do not become transport pathways for oxygen into the substrate. In addition, the substrate carbon is not released, thereby maintaining the mechanical properties of the C/C composite. The appearance of cracks may be associated with the elevated heating and cooling rates during the HVSPS process, because of the differences in the thermal expansion coefficients of SiO_2 (1.0×10^{-6}/°C), SiC (4.0×10^{-6}/°C), and C/C (6.0×10^{-6}/°C). Table 1 shows the thicknesses of the obtained coatings, measured from the sample cross-sections.

Fig. 9 shows the top view of the coating, demonstrating that the coating contains microcracks from thermal expansion but no significant porosity, because the material is very dense from its nanostructural characteristics. Fig. 9(a) shows an area where an image with higher magnification is obtained to confirm the coating nanostructure (Fig. 9(b) and (c)). The spherical grains forming the coating have measured diameters of ~ 39 nm. Nanostructured coatings have superior mechanical and thermal properties compared to those of traditional coatings [44]; such structures can be obtained by the characteristics of the HVSPS process.

3.4. Testing of coatings under ablative conditions

To verify the stability of the coatings, the self-healing ability of SiO_2, and the continued protection of the substrate by the coatings despite the presence of cracks, tests were performed following ASTM E285-80, the standard test method for the oxyacetylene ablation testing of thermal insulation materials [45]. In this test, the samples were held normal to the oxyacetylene torch flame while the pressures of oxygen and acetylene were adjusted to manipulate the mixture composition of the two gases. The oxyacetylene torch was ignited to prevent immediate flame contact with the substrate; the flame was then brought to a standard distance (20 mm) from the substrate. During the test, the samples remained in contact with the flame for 90 s. The temperatures of the sample surfaces were continuously monitored by an infrared pyrometer (Thermalert TX Raytek). The maximum temperature reached during the test was 1800 °C, exceeding the SiO_2 melting temperature of 1700 °C and thereby enabling the evaluation of the self-healing ability of the coatings. Fig. 10 shows images of the samples before (Fig. 10(a)) and after exposure to the hot and oxidizing atmosphere (Fig. 10(b)). In these images, decreases in crack density are observed; that is, the material heals the cracks. Measurements of the areas of the cracks present in the coatings before and after the ablation test show that the cracks before ablation (Fig. 10(a)) occupy 8% of the total image area; after testing, the cracks occupy 1% total (Fig. 10(b)). This result demonstrates that the coating obtained by the HVSPS process has self-healing ability; even after exposure to a hot and oxidizing atmosphere, the coating remains stable and guarantees the protection of the substrate.

4. Conclusions

SiO_2 coatings with SiC gradients were deposited on the surface of C/C composites using the newly developed HVSPS process. The compositions and microstructures of the deposited coatings were characterized by XRD, Raman spectroscopy, FTIR spectroscopy, SEM, and EDS. SiC formation occurred at atmospheric pressure by the reaction of the sprayed material with the substrate, promoted by the thermal and kinetic characteristics of the HVSPS process. SiC was present in all areas of the coatings, but the highest concentration of SiC was located at the substrate/coating interface, avoiding the necessity of a bond coating. XRD showed the formation of a non-crystalline SiO_2 coating, directly related to the high heat transfer between plasma and particles and the low residence time of the particles. In the HVSPS process, the particles were quickly heated and cooled, promoting the formation of non-crystalline structures of ceramic materials. SiO_2 showed self-healing characteristics, able to seal cracks and enhance substrate protection. The self-healing characteristics of the SiO_2 coatings were observed through ablative testing. The results of Raman and FTIR spectral analysis demonstrated the SiO_2/SiC compositional gradients in the coatings. Regarding the microstructural characteristics of the coatings, the formation of cracks from the differences in thermal expansion behaviors of the substrate and coating was observed; however, these cracks did not compromise the coating integrity. The obtained coatings were

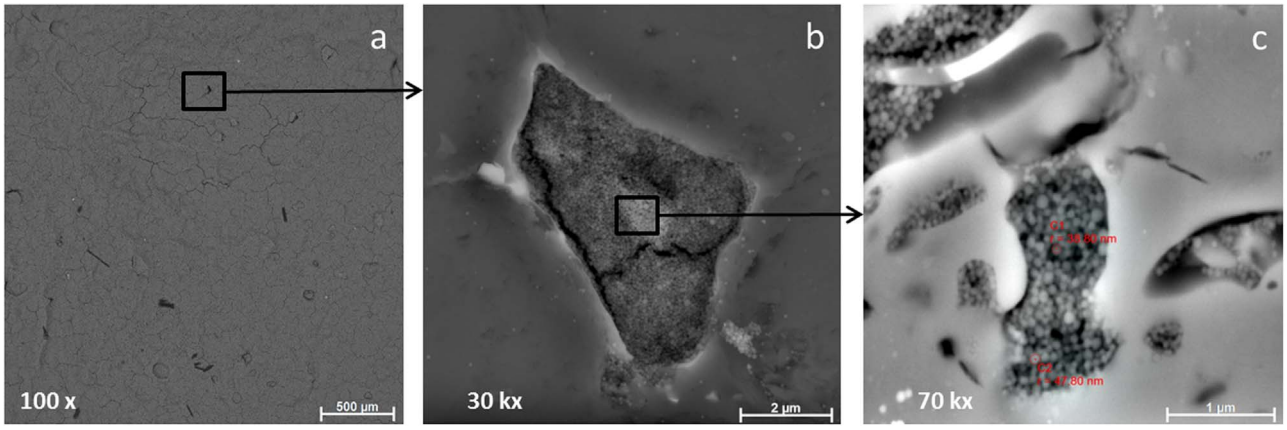

Fig. 9. (a) Top view of the coating, (b) nanostructure of coatings, and (c) particle measurements.

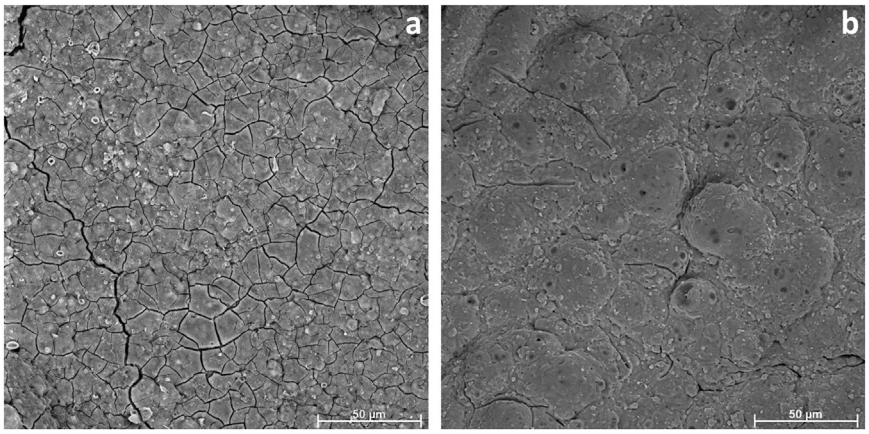

Fig. 10. Coating (a) before and (b) after exposure to the hot and oxidizing atmosphere.

nanostructured with grain sizes of ~ 39 nm, providing lower defect indices, higher strain tolerance, and better porosity distribution, and thereby reduced thermal conductivity and elasticity modulus. These characteristics were directly related to the HVSPS process, demonstrating the increased potential applicability of plasma spray techniques.

Acknowledgements

The authors acknowledge the financial support grant #870484/1997-4 provided by National Council for Scientific and Technological Development (CNPq) and São Paulo Research Foundation (FAPESP) of Brazil.

References

[1] R. Palaninathan, Behavior of carbon-carbon composite under intense heating, Int. J. Aerosp. Eng. 2010 (2010) 1–7, http://dx.doi.org/10.1155/2010/257957.
[2] J.D. Webster, R.J. Day, F.H. Hayes, R. Taylor, M. Westwood, J.D. Webster, R.J. Day, Oxidation protection for carbon fibre composites, J. Mater. Sci. 31 (1996) 1389–1397 ⟨http://link.springer.com/article/10.1007/BF00357844⟩.
[3] J.I. Kim, W.J. Kim, D.J. Choi, J.Y. Park, W.S. Ryu, Design of a C/SiC functionally graded coating for the oxidation protection of C/C composites, Carbon N.Y. 43 (2005) 1749–1757, http://dx.doi.org/10.1016/j.carbon.2005.02.025.
[4] G. Savage, Carbon-Carbon Composites, (1993).
[5] K.N. Lee, Current status of environmental barrier coatings for Si-Based ceramics, Surf. Coat. Technol. 133–134 (2000) 1–7, http://dx.doi.org/10.1016/S0257-8972(00)00889-6.
[6] K.N.U. Lee, Current status of environmental barrier coatings for Si-Based ceramics, Surf. Coat. Technol. (2000) 1–7.
[7] K. Ando, K. Furusawa, K. Takahashi, S. Sato, Crack-healing ability of structural ceramics and a new methodology to guarantee the structural integrity using the ability and proof-test, J. Eur. Ceram. Soc. 25 (2005) 549–558, http://dx.doi.org/10.1016/j.jeurceramsoc.2004.01.027.
[8] T. Engel, G. Kickelbick, Self-healing nanocomposites from silica − polymer core − shell nanoparticles, Polym. Int. (2013), http://dx.doi.org/10.1002/pi.4642.
[9] R. Palaninathan, S. Bindu, Self-healing nanocomposites from silica − polymer core − shell nanoparticles, J. Spacecr. Rockets 42 (2005), http://dx.doi.org/10.2514/1.10710.
[10] A. Kaiser, M. Lobert, R. Telle, Thermal stability of zircon (ZrSiO 4), J. Eur. Ceream. Soc. 28 (2008) 2199–2211, http://dx.doi.org/10.1016/j.jeurceramsoc.2007.12.040.
[11] X. Yao, H. Li, Y. Zhang, H. Wu, X. Qiang, A SiC – Si – ZrB 2 multiphase oxidation protective ceramic coating for SiC-coated carbon/carbon composites, Ceram. Int. 38 (2012) 2095–2100, http://dx.doi.org/10.1016/j.ceramint.2011.10.047.
[12] O. Haibo, L. Cuiyan, H. Jianfeng, C. Liyun, F. Jie, L. Jing, X. Zhanwei, Self-healing ZrB2-SiO2 oxidation resistance coating for SiC coated carbon/carbon composites, Corros. Sci. 110 (2016) 265–272, http://dx.doi.org/10.1016/j.corsci.2016.04.040.
[13] S.S. Hwang, A.L. Vasiliev, N.P. Padture, Improved processing and oxidation-resistance of ZrB2 ultra-high temperature ceramics containing SiC nanodispersoids, Mater. Sci. Eng. A 464 (2007) 216–224, http://dx.doi.org/10.1016/j.msea.2007.03.002.
[14] J. Huang, H. Li, X. Zeng, K. Li, Yttrium silicate oxidation protective coating for SiC coated carbon, Carbon Compos. 32 (2006) 417–421, http://dx.doi.org/10.1016/j.ceramint.2005.03.018.
[15] J. Liu, L. Cao, J. Huang, Y. Xin, W. Yang, J. Fei, C. Yao, Surface & coatings technology A ZrSiO 4/SiC oxidation protective coating for carbon/carbon composites, Surf. Coat. Technol. 206 (2012) 3270–3274, http://dx.doi.org/10.1016/j.surfcoat.2012.01.030.
[16] P. Fauchais, Understanding plasma spraying, J. Phys. D Appl. Phys. 37 (2004) R86–R108, http://dx.doi.org/10.1088/0022-3727/37/9/R02.
[17] P. Fauchais, V. Rat, J.F. Coudert, R. Etchart-Salas, G. Montavon, Operating parameters for suspension and solution plasma-spray coatings, Surf. Coat. Technol. 202 (2008) 4309–4317, http://dx.doi.org/10.1016/j.surfcoat.2008.04.003.
[18] L. Xie, X. Ma, A. Ozturk, E.H. Jordan, N.P. Padture, B.M. Cetegen, D.T. Xiao, M. Gell, Processing parameter effects on solution precursor plasma spray process spray patterns, Surf. Coat. Technol. 183 (2004) 51–61, http://dx.doi.org/10.1016/j.surfcoat.2003.09.071.
[19] P. Fauchais, R. Etchart-Salas, V. Rat, J.F. Coudert, N. Caron, K. Wittmann-Ténèze, Parameters controlling liquid plasma spraying: solutions, sols, or suspensions, J. Therm. Spray. Technol. 17 (2008) 31–59, http://dx.doi.org/10.1007/s11666-007-9152-2.
[20] R.G. Ford, Functionally Graded, n.d.
[21] G. Udupa, S.S. Rao, K.V. Gangadharan, Functionally graded composite materials: an overview, Procedia Mater. Sci. 5 (2014) 1291–1299, http://dx.doi.org/10.1016/j.mspro.2014.07.442.
[22] P. Mi, J. He, Y. Qin, K. Chen, SC, Surf. Coat. Technol. (2016), http://dx.doi.org/10.1016/j.surfcoat.2016.11.033.
[23] X. Dai, D. Yan, Y. Yang, Z. Chu, X. Chen, J. Song, In situ (Al, Cr) 2 O 3 -Cr composite coating fabricated by reactive plasma spraying, Ceram. Int. 43 (2017) 6340–6344, http://dx.doi.org/10.1016/j.ceramint.2017.02.042.
[24] F.R. Caliari, F.S. Miranda, D.A.P. Reis, G.P. Filho, L.I. Charakhovski, A. Essiptchouk, Plasma torch for supersonic plasma spray at atmospheric pressure, J. Mater. Process. Technol. 237 (2016) 351–360, http://dx.doi.org/10.1016/j.jmatprotec.2016.06.027.
[25] Y. Yang, K. Li, Z. Zhao, H. Li, Ablation resistance of HfC-SiC coating prepared by supersonic atmospheric plasma spraying for SiC-coated C/C composites, Ceram. Int. 42 (2016) 4768–4774, http://dx.doi.org/10.1016/j.ceramint.2015.11.161.
[26] X. Qi, G. Zhai, J. Liang, S. Ma, X. Liu, B. Xu, Preparation and characterization of SiC@CNT coaxial nanocables using CNTs as a template, CrystEngComm 16 (2014) 9697–9703, http://dx.doi.org/10.1039/C4CE00693C.
[27] G. Gundiah, G.V. Madhav, A. Govindaraj, M.M. Seikh, C.N.R. Rao, Synthesis and characterization of silicon carbide, silicon oxynitride and silicon nitride nanowires, J. Mater. Chem. 12 (2002) 1606–1611, http://dx.doi.org/10.1039/b200161f.
[28] F. Allaire, L. Parent, S. Dallaire, Production of submicron SiC particles by d.c. thermal plasma: a systematic approach on injection parameters, J. Mater. Sci. 26 (1991) 4160–4165.
[29] F. Abourida, M, Harb, Synthesis and characterization of amorphous silica nanoparticles from aqueous silicates using cationic sulfactants, J. Met. Mater. Miner. 24 (2014) 37–42, http://dx.doi.org/10.14456/jmmm.2014.7.
[30] Y. Yang, K. Li, G. Liu, Z. Zhao, Ablation-resistant composite coating of HfC-TaC-SiC for C/C composites deposited by supersonic atmospheric plasma spraying, vol. 386, 2016, pp. 379–386. ⟨http://doi.org/10.4416/JCST2016-00050⟩.
[31] W.R. Fahrner, Amorphous Silicon/crystalline Silicon Heterojunction Solar Cells, (2011).
[32] T.P. Quinn, Q. Rev. Biol. 80 (2005) 128–129, http://dx.doi.org/10.1086/431094 (Second Edition, Revised and Expanded).
[33] L. Pawlowski, Suspension and solution thermal spray coatings, Surf. Coat. Technol. 203 (2009) 2807–2829, http://dx.doi.org/10.1016/j.surfcoat.2009.03.005.
[34] P.L. Fauchais, J.V.R. Heberlein, M.I. Boulos, Thermal Spray Fundamentals, (2014), http://dx.doi.org/10.1007/978-0-387-68991-3.
[35] A.M. Essiptchouk, F.R. Caliari, F. Miranda, D.A.P. Reis, G. Petraconi, L.I. Charakhosvki, Numerical Modelling of Powder Interaction with Plasma Flow in Tandem-type Plasma Torch, 2015, pp. 10–13.
[36] S.R. Elliott, Medium-range structural order in covalent amorphous solids, Nature 354 (1991) 445–452, http://dx.doi.org/10.1038/354445a0.
[37] D.S. Knight, W.B. White, Characterization of diamond films by Raman spectroscopy, J. Mater. Res. 4 (1989) 385–393, http://dx.doi.org/10.1557/JMR.1989.0385.
[38] H. Hald, Operational limits for reusable space transportation systems due to physical boundaries of C/SiC materials, Aerosp. Sci. Technol. 7 (2003) 551–559, http://dx.doi.org/10.1016/S1270-9638(03)00054-3.
[39] Y.P. Guo, J.C. Zheng, A.T.S. Wee, C.H.A. Huan, K. Li, J.S. Pan, Photoluminescence

studies of SiC nanocrystals embedded in a SiO 2 matrix, Chem. Phys. Lett. 339 (2001) 319–322.
[40] M. Barbouche, R.B. Zaghouani, N.E. Benammar, K. Khirouni, Synthesis and characterization of 3C-SiC by rapid silica carbothermal reduction, Int. J. Adv. Manuf. Technol. (2017) 1339–1345, http://dx.doi.org/10.1007/s00170-016-9838-z.
[41] G. Gundiah, G.V. Madhav, A. Govindaraj, M.M. Seikh, C.N.R. Rao, Synthesis and characterization of silicon carbide, silicon oxynitride and silicon nitride nanowires, J. Mater. Chem. 12 (2002) 1606–1611, http://dx.doi.org/10.1039/b200161f.
[42] A.M.W. Hunt (Ed.), The Oxford Handbook of Archaeological Ceramic Analysis, Oxford University Press, 2016, , http://dx.doi.org/10.1093/oxfordhb/9780199681532.001.0001.
[43] S. van der Zwaag, Routes and mechanisms towards self healing behaviour in engineering materials, Bull. Pol. Acad. Sci. Tech. Sci. 58 (2010) 227–236, http://dx.doi.org/10.2478/v10175-010-0022-6.
[44] Y. Zeng, S.W. Lee, L. Gao, C.X. Ding, Atmospheric plasma sprayed coatings of nanostructured zirconia, J. Eur. Ceram. Soc. 22 (2002) 347–351.
[45] Standard Test Method for Oxyacetylene Ablation Testing of Thermal Insulation Materials, 2015.